



Original research article

Effective algorithmic operational framework for fish texture evaluation in industry: Achieving maturity

D. Dimogianopoulos^a, K. Grigorakis^{b,*}^a University of West Attica, Department of Industrial Design and Production Engineering, Athens, 12244, Greece^b Hellenic Center for Marine Research, Institute of Marine Biology, Biotechnology & Aquaculture, Anavyssos, Attica, 19013, Greece

ARTICLE INFO

Keywords:

Texture assessment
Freshness evaluation
Sea bass
Physics-based model
Closed-form analytical solution

ABSTRACT

Reliable, nondestructive fish freshness evaluation applicable during fish commercialization has been continuously pursued by scientists and industry. Taking into account that fish texture is primarily affected even at early stages of post-mortem storage, a relevant nondestructive testing framework for rapid textural assessment of fish freshness was developed in the past. Herein, an algorithm operating within the aforementioned framework and optimized for use in industrial environments is proposed. Sea bass (*Dicentrarchus labrax*) both freshly killed and stored on ice for 6 days have been used for comparative testing. The fish is part of a system, which is vibration-tested via a new testing protocol designed for easy implementation and robustness to noise. At the same time, a new closed-form analytical expression for the system response to the specific testing is computed and used along with experimental data, for obtaining specific mechanical (thus muscle-structural) characteristics of fish flesh. This computation is designed to only require readily available routines found in most relevant software. The algorithmic operational framework has been used in two different test setups (a custom-built test rig and a prototype device), with results following remarkably similar trends, clearly discriminating different textural (thus freshness) characteristics, and consequently validating the proposed approach.

1. Introduction

Regardless of the perspective under which the term “fish quality” is defined, freshness is always one of its capital components. Whether quality is defined under the form of the four terms of security, healthiness, satisfaction and serviceability (Listrat et al., 2016), or by the four pillars of freshness, safety, traceability and authentication (Freitas et al., 2020), or even under the narrower scope of a combination of nutritional, microbiological, biochemical, and physicochemical characteristics (Hassoun & Karoui, 2017), freshness is always a major quality determinant; this is due to the highly perishable nature of this food item.

Therefore, besides traditional sensory, microbiological and physicochemical analyses used for describing freshness reduction or spoilage of fish, a large effort has been undertaken in order to develop methods evaluating fish freshness in a rapid way and ideally without destruction of the samples under examination (Cheng et al., 2015; Hassoun; Karoui, 2017). These include refractive index techniques, colorimetric or other sensor technologies, such as the electronic nose, gas sensors, semi-conducting metaloxide sensors, or spectroscopy methods, namely infrared - IR or near infrared reflectance - NIR, visible spectroscopy,

electrochemical impedance spectroscopy -EIS and fluorescence spectroscopy. These techniques have been comprehensively reviewed in recent literature (Cheng et al., 2015; Hassoun; Karoui, 2017).

Fish texture is one of the first features undergoing post-mortem changes in fish due to the evolution of rigor-mortis even within hours after slaughtering (Huss, 1988, p. 134). This makes texture a valuable feature for determining early post-mortem changes even at stages when other feature changes remain unnoticed. However, textural assessments of freshness are mostly exhausted in Texture Profile Analysis-TPA and therefore involve scientific instrumentology and various tests of increased complexity (Hassoun; Karoui, 2017). Some indirect approaches, evaluating texture by means of combination of dynamometric measurements of hardness (Zwick 1.0 Universal Testing Machine, Zwick/Roell Testing System, Kennesaw, GA, USA) with spectrophotometric image analysis have also obtained reliable results in discriminating textural differences based on freshness and origin of fish (Costa et al., 2011).

Along such guidelines, the authors have proposed a nondestructive testing framework for rapid textural assessment of fish freshness, and pursued its development over several years (Grigorakis &

* Corresponding author.

E-mail address: kgrigo@hcmr.gr (K. Grigorakis).<https://doi.org/10.1016/j.aaf.2020.10.001>

Received 4 May 2020; Received in revised form 1 October 2020; Accepted 8 October 2020

Available online 16 October 2020

2468-550X/© 2020 Shanghai Ocean University.

Published by Elsevier B.V. This is an open access article under the CC BY-NC-ND license

[\(http://creativecommons.org/licenses/by-nc-nd/4.0/\)](http://creativecommons.org/licenses/by-nc-nd/4.0/).

Dimogianopoulos, 2010) (Dimogianopoulos & Grigorakis, 2011, 2014, 2017). The initial effort (Grigorakis & Dimogianopoulos, 2010) consisted in assessing specific fish mechanical properties related to key physical characteristics (viscoelasticity, springiness and so on) via fault diagnosis principles traditionally applied to mechanical systems. The fish was considered as part of a system including mechanical and electrical components, which was subjected to a step-like externally imposed load. The system response was analyzed for evaluating specific attributes, which were intimately related to fish textural changes. Over the years, effort has been invested in fine-tuning the system's definition and modelling, initially by using a stochastic modelling framework for accurately evaluating the system response in presence of noise (Dimogianopoulos & Grigorakis, 2011) or for alleviating the influence of fish mass variation on system response (Dimogianopoulos & Grigorakis, 2014). Both approaches functioned well in the context of lab experiment practice. In view of the framework's promising results, effort was subsequently invested in simplifying the experimental and modelling procedure by proposing semi-static (instead of vibration-like) experimental excitation along with delivering a complete closed-form mathematical expression of the system response for this excitation (Dimogianopoulos & Grigorakis, 2017). The aim was to analytically compute both stiffness and viscoelastic textural attributes of the fish and thereby achieve quantitative monitoring of alterations attributable to freshness changes. Again, the approach yielded successful results in lab environment, where measurement noise could be successfully dealt with. Nonetheless, owing to the authors' participation in EU-funded FutureEUAqua research project, emphasis had shifted towards applying this nondestructive textural assessment framework for use principally within an industrial environment. To this end, further work had to be carried out along two main directions. First, for simplifying the testing protocol and the algorithmic operation of the framework (thus facilitating its implementation), while minimizing the effects of noise in measurements used for fish texture evaluation. Then for developing a prototype device capable of applying various nondestructive methodologies and evaluating the fish texture and freshness. An indicative but not exclusive example are the aforementioned methodologies postulated over the last years.

The aim of the current study is to propose a less restrictive testing protocol along with a simplified algorithmic operation of the nondestructive texture evaluation framework, for achieving robust operation under noisy measurements and delivering results with only basic user intervention in data processing. In other words, the aim is to achieve maturity as far as the framework's implementation in industrial environments is concerned. The fish is still integrated in a mechanical structure (referred to as system), but most limitations of the testing procedure have now been removed, so that favorable signal-to-noise values for the experimental data may be recordable. At the same time, the development of a new physics-based system model provides an accurate closed-form analytical expression for the system response. Using the latter along with experimental data, one may easily compute specific characteristics of fish flesh related to viscoelasticity, springiness and so on. Doing so, no longer requires specific skills (in stochastic identification, for instance) from the user. The use of conventional curve-fitting routines, found in most relevant software such as MATLAB®, is the main requirement. Lastly, given that a custom-built test rig (developed over the years) was available and that the aforementioned prototype device for texture evaluation is being developed, the validation of the framework in both setups is presented. The paper is organized as follows: In the Introduction, a quick overview of relevant literature along with the current study's contribution is presented. The section entitled "Materials and Methods" provides details on the tested fish, and a comprehensive analysis of the framework algorithmic operation, namely the testing protocol, the physics-based system model and the closed-form expression of its response to testing. In section "Results and Discussion" results of the application of the framework on six fish of different freshness state are shown and commented upon.

2. Materials and methods

2.1. Fish

Common sea bass (*Dicentrarchus labrax*) of commercial size was used for the freshness evaluation experiments. Fish originated from the experimental facilities of HCMR (Ag. Kosmas, Attika), reared in a closed recirculated system with cement tanks of 1 m³ and fed with a commercial diet. Fish rearing complied with the respective European Union (EU) Council Directive 98/58/EC, concerning the protection of animals kept for farming purposes and the European Commission (EC) recommendation on the welfare of farmed fish. Fish were slaughtered by custom industrial slaughter method of ice-water immersion, thus complying with the recommendations of the Opinion of the Scientific Panel on Animal Health and Welfare (AHAW), on a request from the Commission related to Species-specific welfare aspects of the main systems of stunning and killing of farmed seabass and seabream (European Food Safety Authority, 2009). Fish were slaughtered in two time-intervals within 6 days in order to allow simultaneous availability of freshly killed individuals and individuals stored on ice (0°C) for 6 days. The individual characteristics of the studied fish appear in Table 1.

2.2. Design of the testing protocol

The design of the testing protocol is quite similar to that in previous efforts (Grigorakis & Dimogianopoulos, 2010), (Dimogianopoulos & Grigorakis, 2011, 2014 and 2017), but significant changes have been undertaken in the algorithmic framework used for processing the experimental data and performing the diagnostic task. In essence, the fish is placed onto a tray suspended by a spring with constant K_b , and free to oscillate vertically under external excitation, as shown in Fig. 1. A block of specific mass is.

Released at a specific height above the fish surface, so that it drops freely and hits the fish on the tray, thus exercising a vertical loading force $f(t)$, as also shown in Fig. 1. Following the excitation, the system consisting of tray, fish and the block, oscillates under the load $f(t)$ until it stops a few seconds later. Care is taken to place the fish at the same position on the tray and to ensure that the block hits the fish at roughly the same dorsal area of fish at each test.

In this study, two distinctive setups have been used for experimental testing. The first one has been developed over the last few years and is an evolution of that used in (Dimogianopoulos & Grigorakis, 2014). It involves a custom-built rig with a free vertically moving, spring-suspended wooden tray upon which the fish is placed. The spring is connected to an electronic force gauge for measuring the response $fg(t) = Kg \cdot xw(t)$ exercised by the ground when the system is under load $f(t)$. A small plastic hammer acts as the block exercising the loading force $f(t)$. The second one is the outcome of joint efforts of partners in FutureEUAqua project, funded by the European Union (see Acknowledgements). Development of a Texture Evaluation (TE) device, is currently being finalized, meaning that technical details are confidential and, as such, cannot be disclosed. Since the current study is concerned with the definition and validation of the algorithmic operational framework (rather than the device for its implementation) for evaluating fish texture, it may only be stated that the TE is purposely designed to work

Table 1
The fish tested, their characteristics and the setup used for testing.

Fish	Mass (gr)	Days killed	Test setup
F_1	240 ± 5	0	custom-built rig
F_2	235 ± 5	6	custom-built rig
F_3	255 ± 5	0	TE
F_4	245 ± 5	0	TE
F_5	255 ± 5	6	TE
F_6	250 ± 5	6	TE

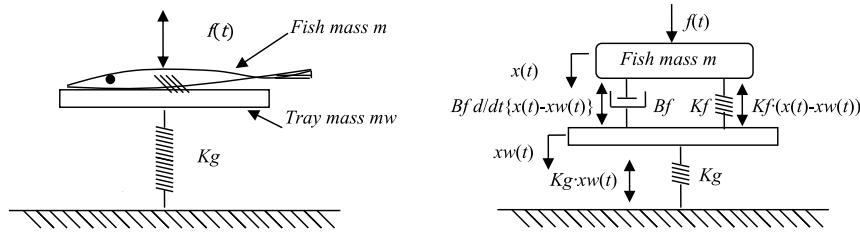


Fig. 1. The principle of operation of the experimental testing (left) and its representation by means of the Kelvin-Voigt fish model (involving fish mass m , damping element Bf and spring element Kf) and a spring Kg (right).

under a variety of loading protocols including (but not limited to) that presented herein. As such, it has been used to check results for relevance with respect to those obtained from the custom-built rig.

2.3. Algorithmic framework for fish texture evaluation

According to the Kelvin-Voigt model, the fish mass m is considered as

$$Fg(s) = Kg \cdot Xw(s) \tag{6}$$

with s the Laplace domain argument, and $R(s)$ denoting the transformed quantity $r(t)$ in the Laplace domain. Combining (4), (5) and (6) and performing some standard calculus one may obtain the transfer function $Fg(s)/F(s)$:

$$\frac{Fg(s)}{F(s)} = \frac{Kg \cdot [Bf \cdot s + Kf]}{m \cdot mw \cdot s^4 + [Bf \cdot m + Bf \cdot mw] \cdot s^3 + [(Kf + Kg) \cdot m + mw \cdot Kf] \cdot s^2 + Kg \cdot Bf \cdot s + Kg \cdot Kf} \tag{7}$$

a point mass suspended by a set of one damping and one spring elements in parallel, with constants Bf and Kf , respectively. The damping element is used for modelling viscoelasticity of fish flesh, namely its opposing force to a deformation imposed at steady speed. The spring element is used for modelling the flesh elasticity and springiness, namely its opposing force to an external load and its capacity of readmitting its initial form when the load is removed. During loading from an external force $f(t)$ the fish flesh reacts by opposing a force by the spring element equal to $Kf \cdot (x(t) - xw(t))$ and another by the damping element equal to $Bf \cdot d/dt[x(t) - xw(t)]$, with the operator d/dt denoting first order derivative with respect to time. The ground also reacts by opposing a force $Fg(t)$ equal to $Kg \cdot xw(t)$. From Newton's law one may write for the fish and the tray, respectively:

$$-Kf \cdot [x(t) - xw(t)] - Bf \cdot \frac{d}{dt}[x(t) - xw(t)] + f(t) = m \cdot \frac{d^2}{dt^2}x(t) \tag{1}$$

$$Kf \cdot [x(t) - xw(t)] + Bf \cdot \frac{d}{dt}[x(t) - xw(t)] - Kg \cdot xw(t) = mw \cdot \frac{d^2}{dt^2}xw(t) \tag{2}$$

Finally, the ground responds to fish loading by a force $Fg(t)$ as follows:

$$Fg(t) = Kg \cdot xw(t) \tag{3}$$

with $d^2/dt^2[x(t)]$ the second order time derivative of $x(t)$ and the displacements $x(t)$ and $xw(t)$ measured from the equilibrium point. Following some standard methodology as found in System Theory (see Dorf & Bishop, 2010), by applying Laplace transform on (1), (2) and (3) and rearranging terms, one has:

$$m \cdot s^2 \cdot X(s) + Bf \cdot s \cdot [X(s) - Xw(s)] + Kf \cdot [X(s) - Xw(s)] = F(s) \tag{4}$$

$$mw \cdot s^2 \cdot X(s) - Bf \cdot s \cdot [X(s) - Xw(s)] - Kf \cdot [X(s) - Xw(s)] + Kg \cdot Xw(s) = 0 \tag{5}$$

Equation (7) is a function relating the ground response (effect) to fish loading (cause) in the Laplace domain. The denominator features a maximum order of s equal to 4 and the numerator has a maximum order of s equal to 1. Setting the denominator polynomial equal to zero and solving for s yields four solutions referred to as the *system poles*, whereas applying the same procedure to the numerator yields one solution referred to as the *system zero*.

In general, if quantities Bf , Kf , Kg , m , mw are treated as variables, obtaining an analytical closed-form expression for $Fg(s)$ (in view of ultimately computing the function $fg(t)$ in the time domain via the application of the inverse Laplace transform) is a very complex task. In relevant textbooks (Dorf & Bishop, 2010) such analytical solutions are only available for systems of up to 2nd order under specific loading functions $f(t)$. Nonetheless, one may considerably simplify the task of $f(t)$ calculation by proceeding as follows. If the tray mass mw is very small and in any case considerably lower than m , then (7) may be simplified as follows:

$$\frac{Fg(s)}{F(s)} = \frac{Kg \cdot [Bf \cdot s + Kf]}{[Bf \cdot m] \cdot s^3 + [(Kf + Kg) \cdot m] \cdot s^2 + [Kg \cdot Bf] \cdot s + Kg \cdot Kf} \tag{8}$$

This assumption is not unreasonable since m designates the oscillating mass following $f(t)$ application. The latter is normally carried out by means of a block dropping onto the fish from a specific height, meaning that the total oscillating mass m includes that of the fish plus the block. Then, m is, by all means, quite larger than mw . Adding and subtracting $[Bf \cdot m] \cdot s^3 + [(Kf + Kg) \cdot m] \cdot s^2$ in the numerator of (8) yields:

$$\frac{Fg(s)}{F(s)} = 1 - \frac{s^2 \cdot [Bf \cdot m \cdot s + (Kf + Kg) \cdot m]}{[Bf \cdot m] \cdot s^3 + [(Kf + Kg) \cdot m] \cdot s^2 + [Kg \cdot Bf] \cdot s + Kg \cdot Kf} \tag{9}$$

Equation (9) states that the ground response $Fg(s)$ is equal to the load $F(s)$ minus the response to $F(s)$ of the 3rd order subsystem

$$P(s) = \frac{s^2 \cdot [Bf \cdot m \cdot s + (Kf + Kg) \cdot m]}{[Bf \cdot m] \cdot s^3 + [(Kf + Kg) \cdot m] \cdot s^2 + [Kg \cdot Bf] \cdot s + Kg \cdot Kf} \tag{10}$$

The subsystem $P(s)$ has three poles, one real and two complex ones. Setting $s = -Kf/Bf$ in the denominator of (10) yields $m \cdot Kg \cdot Kf^2/Bf^2 > 0$, whereas setting $s = -(Kf + Kg)/Bf$ [which is equal to the system zero in (10)] yields $-Kg^2 < 0$. Hence, one of the three poles of (10) admits value between $-(Kf + Kg)/Bf$ and $-Kf/Bf$, or in other terms:

$$s = -\frac{Kf + n \cdot Kg}{Bf}, \quad 0 < n < 1 \tag{11}$$

Replacing (11) into the denominator of (10) yields:

$$\frac{m}{Bf^2} (1 - n) \cdot (n \cdot Kg + Kf)^2 - n \cdot Kg = 0 \tag{12}$$

Equation (9) may be rewritten as:

$$\frac{Fg(s)}{F(s)} = 1 - \frac{s^2 \cdot \left[s + \frac{Kf + Kg}{Bf} \right]}{s^3 + \frac{Kf + Kg}{Bf} \cdot s^2 + \frac{Kg}{m} \cdot s + \frac{Kg \cdot Kf}{Bf \cdot m}} \tag{13}$$

Knowing that the denominator in (13) has the pole defined in (11), one may write (13):

$$\frac{Fg(s)}{F(s)} = 1 - \frac{s^2 \cdot \left[s + \frac{Kf + Kg}{Bf} \right]}{\left(s + \frac{Kf + n \cdot Kg}{Bf} \right) \cdot \left[s^2 + \frac{(1 - n) \cdot Kg}{Bf} \cdot s + \frac{Kg}{m} - \frac{(1 - n) \cdot Kg}{Bf^2} \cdot (Kf + n \cdot Kg) \right]} + \varepsilon \tag{14}$$

$$\varepsilon = \frac{n \cdot Kg^2}{Bf \cdot m} + \frac{(1 - n) \cdot Kg}{Bf^3} \cdot (Kf + n \cdot Kg)^2 \rightarrow 0$$

since the expression of ε in (14) is a slightly different version of (12). Furthermore, another realistic remark is that $Kf \gg Kg$, meaning that the fish is considerably stiffer than the spring used to support the tray. In that case, (14) becomes approximately equal to:

$$\frac{Fg(s)}{F(s)} = 1 - \frac{s^2}{s^2 + \frac{(1 - n) \cdot Kg}{Bf} \cdot s + \frac{Kg}{m} - \frac{(1 - n) \cdot Kg}{Bf^2} \cdot (Kf + n \cdot Kg)} \tag{15}$$

since the term $[s + (Kf + Kg)/Bf]$ in the numerator is approximately cancelled by $[s + (Kf + n \cdot Kg)/Bf]$ in the denominator of (14). From (15) one may write:

$$Fg(s) = F(s) - s \cdot \frac{1}{\omega n^2} \cdot \frac{\omega n^2}{s^2 + 2 \cdot \zeta \cdot \omega n \cdot s + \omega n^2} \cdot s \cdot F(s) \tag{16}$$

with

$$\zeta = \frac{1}{2} \cdot \frac{(1 - n) \cdot Kg}{Bf \cdot \sqrt{\frac{Kg}{m} - \frac{(1 - n) \cdot Kg}{Bf^2} \cdot (Kf + n \cdot Kg)}}, \quad \omega n = \sqrt{\frac{Kg}{m} - \frac{(1 - n) \cdot Kg}{Bf^2} \cdot (Kf + n \cdot Kg)} \tag{17}$$

$$fg(t) = A + A \cdot \left[\frac{\zeta}{\sqrt{1 - \zeta^2}} \cdot e^{-\zeta \cdot \omega n \cdot t} \cdot \sin(\omega n \cdot \sqrt{1 - \zeta^2} \cdot t) - e^{-\zeta \cdot \omega n \cdot t} \cdot \cos(\omega n \cdot \sqrt{1 - \zeta^2} \cdot t) \right] \tag{21}$$

where ζ and ωn are the damping factor and natural frequency of the 2nd order subsystem in (15) (see Dorf & Bishop, 2010).

If the loading function has a step form, meaning that $f(t) = A$ for $t > 0$, then $F(s) = A/s$, as shown in any table of Laplace transforms of standard functions. Then $s \cdot F(s)$ in (16) corresponds to the impulse function

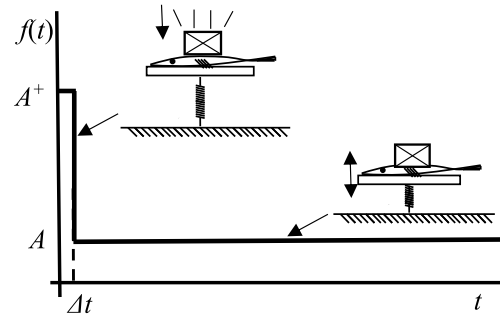


Fig. 2. The loading profile $f(t)$ involving a peak force A^+ during the brief interval Δt of the block hitting the fish, followed by the constant weight A from the group of fish and block getting to oscillate.

multiplied by A , and in (16) the term

$$H(s) = \frac{1}{\omega n^2} \cdot \frac{\omega n^2}{s^2 + 2 \cdot \zeta \cdot \omega n \cdot s + \omega n^2} \cdot s \cdot F(s) = G(s) \cdot s \cdot F(s) \tag{18}$$

is essentially the impulse response of the 2nd order system $G(s)$, as defined in (18), multiplied by A . In other words, (16) essentially states that the response function $Fg(s)$ is obtained if one subtracts the impulse response (multiplied by A) of $G(s)$ defined in (18) from the load function $F(s) = A/s$. The same is valid in the time domain, namely:

$$fg(t) = A - A \cdot \frac{d}{dt} [\text{impulse response of } G(s)] \tag{19}$$

From (Dorf & Bishop, 2010) it is known that the impulse response $h(t)$ of $G(s)$ in the time domain is:

$$h(t) = \frac{1}{\omega n \cdot \sqrt{1 - \zeta^2}} \cdot e^{-\zeta \cdot \omega n \cdot t} \cdot \sin(\omega n \cdot \sqrt{1 - \zeta^2} \cdot t) \tag{20}$$

with ζ and ωn as in (17). Thus, using (20) to perform standard calculus in (19) one obtains:

This is a closed-form analytical solution for the response $fg(t)$ to a step load $f(t) = A$, exercised to the system modelled as in (8).

However, the real profile of the load $f(t)$ may be far from matching a step function. In fact, released from a specific height, the block hits the

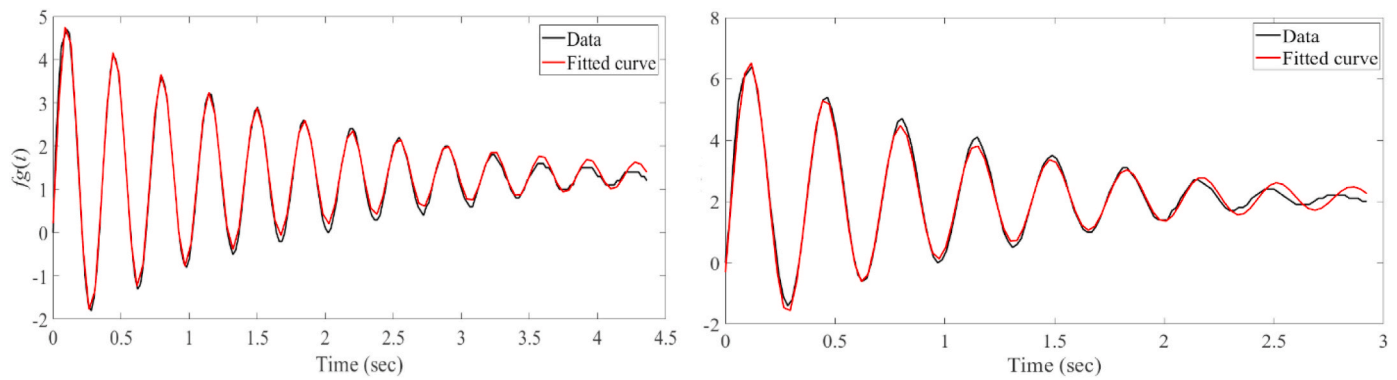


Fig. 3. Typical response signal $f_g(t)$ from test run (in black) with the custom-built rig (left) and the TE (right) and curves fitted (in red) showing almost perfect match except for the last (settling) signal part. (For interpretation of the references to color in this figure legend, the reader is referred to the Web version of this article.)

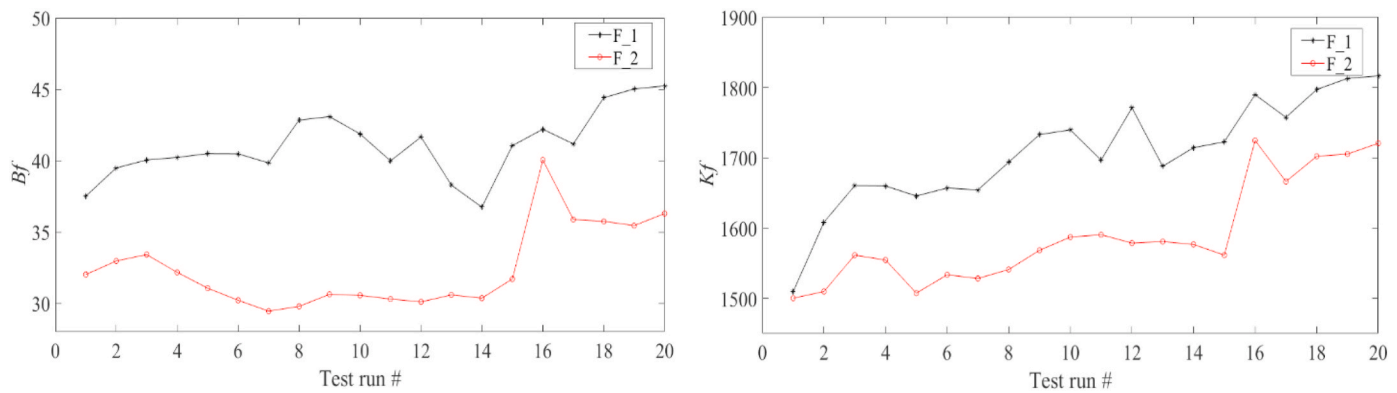


Fig. 4. Values of B_f (left) and K_f (right) for fish F_1 and F_2 computed using data from 20 test runs per fish with the custom-built test rig.

fish surface, thus transmitting its kinetic energy to the fish during the (obviously very brief) time interval of the shock. Following this instant energy transmission, the mass of fish and block on the tray starts oscillating until it stops a few seconds later. Hence, there is a high peak force during the short shock interval, followed by a constant force equal to the weight of the added mass of the block and the fish getting to oscillate, as in Fig. 2. The higher the initial height of release of the block, the more significant the force peak during the short time interval that the collision takes place. In previous work of the authors (in 2010, 2011, 2012 and 2014), care has been taken to drop the block from as low above the fish surface as possible in order to avoid a significant force peak during the collision, as this would result in an $f(t)$ profile significantly different to a step function. The immediate result of this was that, unless the lab equipment had been carefully optimized, the recorded response signal $f_g(t)$ could suffer from noise in the measured values making their exploitation quite challenging. This was particularly true in (Grigorakis & Dimogianopoulos, 2010), where only specific values (those corresponding to the overshoot and settling time) of the response data recorded had to be used for diagnostic purposes.

Careful frequency analysis and filtering of the response data signal could provide relatively accurate measurement of the required values, but this requires signal processing expertise and is often not applicable in an industrial environment. In subsequent work (Dimogianopoulos & Grigorakis, 2011, 2014, 2017) a stochastic framework was used to accommodate the potentially significant noise in measurements. Even though the increased complexity in the algorithmic design (mainly related to identifying a suitable system model) was acceptable in the context of a lab environment and yielded good performance, it could also prove problematic in an industrial environment, where simplicity is the prerequisite to robustness. In view of this, effort was invested in a subsequent work (Dimogianopoulos & Grigorakis, 2017) to apply a

different testing protocol, where the excitation was applied following a ramp-like function. The gradually increasing load of the fish alleviated the problem of the initial collision force peak, but introduced again problems with low signal-to-noise ratio over the initial instants of load application. Again, this problem could be mastered by means of careful handling of the load feed, but this solution required a specifically trained user for carrying out the experiments. This could not always be the case in an industrial environment. Thus, the optimal solution would be to retain and amplify the initial loading application of a block released above the fish by removing restrictions on the release height, as this would allow for obtaining satisfactory signal-to-noise ratios for the recorded response data. If one wished to avoid working within a stochastic framework, an effective solution was to develop a sufficiently accurate closed-form analytical formula of the response data and use it for fitting curves (in a least-squares context) on data recorded during the experiment [as in (Dimogianopoulos & Grigorakis, 2017)], instead of just using specific data values [as in (Grigorakis & Dimogianopoulos, 2010)].

Hence, let $t = 0$ be time of the block meeting the fish surface, thus creating the force A^+ . The shock has a very brief duration of Δt seconds, with the group of fish and block starting to oscillate thereafter. At time $t = 0 + \Delta t$ the force value has settled to A , which is known and equal to the weight of the fish and block. The value A^+ is obviously unknown and should probably be considered as quite variable, had Δt been significant. In the current case of Δt being very short, one may as well consider that A^+ admits a constant value, which could very well be the mean value of the real collision force over Δt . Then, the (short width) pulse with magnitude A^+ over a time interval Δt in Fig. 2 may be modelled as a step function admitting a value A^+ at $t = 0$ and another admitting a value equal to $-A^+$ at $t = 0 + \Delta t$. At $t > 0 + \Delta t$, $f(t) = A$. Then, if $u(t)$ is the unit step function, meaning that $u(t) = 1$ for all $t \geq 0$, the function $f(t)$ has the

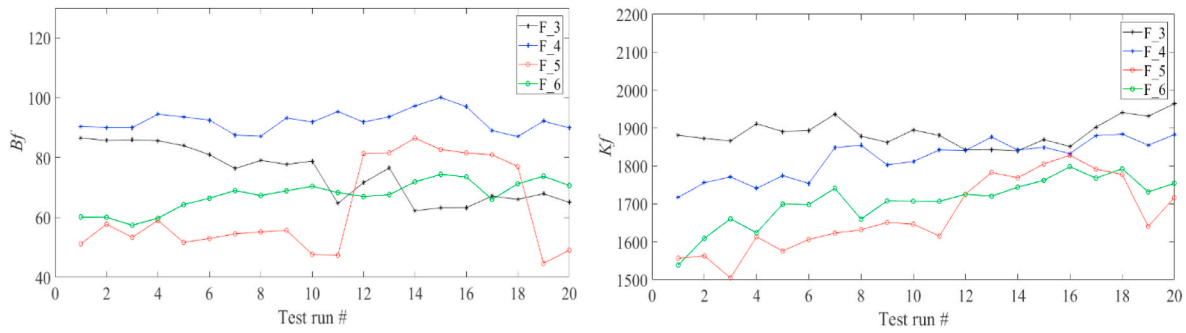


Fig. 5. Values of Bf (left) and Kf (right) for fish F_3 – F_6 computed using data from 20 test runs per fish with the TE.

Table 2

Mean and standard deviation for Bf and Kf computed with tests from the custom-built rig.

	Bf mean for 20 runs (for 15 runs)	Bf std for 20 runs (for 15 runs)	Kf mean for 20 runs (for 15 runs)	Kf std for 20 runs (for 15 runs)
F_1	41.0768 (40.2340)	2.2988 (1.7839)	1706.5 (1677)	76 (62.9)
F_2	32.4380 (31.0237)	2.8452 (1.1749)	1590.1 (1552.1)	73 (30.3)

Table 3

Mean and standard deviation for Bf and Kf computed with test data from the TE.

	Bf mean for 20 runs (for 10 runs)	Bf std for 20 runs (for 10 runs)	Kf mean for 20 runs (for 10 runs)	Kf std for 20 runs (for 10 runs)
F_3	74.4265 (82.0681)	8.8229 (3.9161)	1887.7 (1888.8)	35 (22.4)
F_4	92.2036 (91.0761)	3.5074 (2.4942)	1820.8 (1783.1)	51.6 (45.4)
F_5	62.5873 (53.9109)	14.8277 (3.3021)	1671.3 (1597.3)	95.6 (46.4)
F_6	67.4064 (64.3753)	4.9376 (4.6769)	1707.5 (1664.8)	63.8 (60.1)

following form:

$$f(t) = A^+ \cdot u(t) - A^+ \cdot u(t - \Delta t) + A \cdot u(t - \Delta t) \tag{22}$$

Since the system is linear with a transfer function given by (15), according to the superposition principle of linear systems (Dorf & Bishop, 2010), the system response $fg(t)$ to the input $f(t)$, comprising of the three constituents in (22), will be equal to the sum (superposition) of the system responses to each constituent, namely:

$$fg(t) = fg_{A^+}(t) - fg_{A^+}(t - \Delta t) + fg_A(t - \Delta t) \tag{23}$$

with quantities in (23) corresponding to the system responses to step inputs $A^+ \cdot u(t)$, $-A^+ \cdot u(t - \Delta t)$ and $A \cdot u(t - \Delta t)$, computed by repeatedly using (21):

$$fg_{A^+}(t) = A^+ \cdot u(t) + A^+ \cdot \left[\frac{\zeta}{\sqrt{1 - \zeta^2}} \cdot e^{-\zeta \omega_n t} \cdot \sin(\omega_n \sqrt{1 - \zeta^2} \cdot t) - e^{-\zeta \omega_n t} \cdot \cos(\omega_n \sqrt{1 - \zeta^2} \cdot t) \right] \cdot u(t) \tag{24}$$

$$fg_{A^+}(t - \Delta t) = A^+ \cdot u(t - \Delta t) + A^+ \cdot \left[\frac{\zeta}{\sqrt{1 - \zeta^2}} \cdot e^{-\zeta \omega_n (t - \Delta t)} \cdot \sin(\omega_n \sqrt{1 - \zeta^2} \cdot (t - \Delta t)) - e^{-\zeta \omega_n (t - \Delta t)} \cdot \cos(\omega_n \sqrt{1 - \zeta^2} \cdot (t - \Delta t)) \right] \cdot u(t - \Delta t) \tag{25}$$



Fig. 6. Error-bars for Bf (top) and Kf (bottom) for fish F_1, F_2 computed using data from test runs #1 - #15 with the custom-built rig.

$$fg_A(t - \Delta t) = A \cdot u(t - \Delta t) + A \cdot \left[\frac{\zeta}{\sqrt{1 - \zeta^2}} \cdot e^{-\zeta \cdot \omega n \cdot (t - \Delta t)} \cdot \sin(\omega n \cdot \sqrt{1 - \zeta^2} \cdot (t - \Delta t)) - e^{-\zeta \cdot \omega n \cdot (t - \Delta t)} \cdot \cos(\omega n \cdot \sqrt{1 - \zeta^2} \cdot (t - \Delta t)) \right] \cdot u(t - \Delta t) \tag{26}$$

Equations (23–26) describe the complete system response $fg(t)$ to the input force $f(t)$ in (22), as shown in Fig. 2. For instance, if $0 < t \leq 0 + \Delta t$, then in (23) the term including $\sin(\cdot) \rightarrow 0$, the term involving $\cos(\cdot) = \mu(t)$, with $0 < \mu(t) < 1$, whereas the quantities in (25) and (26) are equal to zero. Thus, one has $fg(t) = A^+ - A^+ \cdot \mu = A^+ \cdot (1 - \mu)$ which is a small positive quantity. On the other hand, if $t > 0 + \Delta t$, from (23)-(26) one has:

$$fg(t) = A + \frac{\zeta}{\sqrt{1 - \zeta^2}} \cdot e^{-\zeta \cdot \omega n \cdot t} \cdot \left[A^+ \cdot \sin(\omega n \cdot \sqrt{1 - \zeta^2} \cdot t) - A^+ \cdot e^{\zeta \cdot \omega n \cdot \Delta t} \cdot \sin(\omega n \cdot \sqrt{1 - \zeta^2} \cdot (t - \Delta t)) + A^+ \cdot e^{\zeta \cdot \omega n \cdot \Delta t} \cdot \sin(\omega n \cdot \sqrt{1 - \zeta^2} \cdot (t - \Delta t)) \right] - e^{-\zeta \cdot \omega n \cdot t} \cdot \left[A^+ \cdot \cos(\omega n \cdot \sqrt{1 - \zeta^2} \cdot t) - A^+ \cdot e^{\zeta \cdot \omega n \cdot \Delta t} \cdot \cos(\omega n \cdot \sqrt{1 - \zeta^2} \cdot (t - \Delta t)) + A^+ \cdot e^{\zeta \cdot \omega n \cdot \Delta t} \cdot \cos(\omega n \cdot \sqrt{1 - \zeta^2} \cdot (t - \Delta t)) \right] \tag{27}$$

Hence, if measured test values for $fg(t)$ are available, then:

- One may use Equations (23–26) along with least-squares curve-fitting algorithms (readily available in dedicated software) to estimate values for ζ and ωn .
- Using (12) and (17), one may easily compute constants n , B_f and K_f for the tested fish, by solving the set of these three equations, again using any relevant routine in dedicated software.

Note that the data fitting process means that noise in measurement is not as significant a problem as in (Grigorakis & Dimogianopoulos, 2010) where only specific $fg(t)$ values were used and had to be precisely known. At the same time, no stochastic system modelling and identification (and the associated expertise from the user) are needed for tolerating noise, as in (Dimogianopoulos & Grigorakis, 2011, 2014, 2017).

3. Results and discussion

As previously stated (subsection 2.3), tests have been conducted with two setups, namely the custom-built rig and the TE whose development is currently being finalized. Therefore, even though the algorithmic framework can be shared, there are key parameters (the block mass and the spring constant K_b , to name but a few) which could never admit the same values in the two test setups for technical reasons. Then, obviously results from testing with the custom-built rig should be qualitatively comparable to those from the TE, meaning that trends in B_f and K_f should be the same between fresh and 6-day-old fish irrespectively of the test setup. The testing procedure involved 20 runs for each fish, with both setups. Initial block release height was set to 3 cm in the custom-built rig, which was the maximum allowable height due to technical.

Limitations. In the TE case, no such limitations were present, hence a more substantial initial block release height of 4 cm was selected. Recording of $fg(t)$ data was carried out at 50 Hz.

Tests were conducted on two separate occasions. First, fish F_1 and

F_2 were tested with the custom-built rig. Some days later, fish F_3-F_6 were tested by means of the TE (Table 1). Testing on different dates was opted for practical reasons. Sequentially testing the same fish with both setups (hence, at the same date) would be impossible, since this would violate the requirement for having a fish of comparable initial condition before each set of 20 test runs.

Fig. 3 presents the recorded $fg(t)$ response for the custom-built rig (left) and the TE (right). The recorded data are presented in black, whereas the red lines show the simulated curve using Equations

(23–26), after performing the least-squares curve-fitting process and the estimation of ζ and ωn values (see subsection 2.3). It is obvious that the representation in (23)-(26) produces curves which essentially match those from experimental data with both setups, with slight differences only notable at the part of the curve settling down. The associated values for B_f and K_f (computed using (17) using the estimated ζ and ωn values-see subsection 2.3) are presented in Fig. 4 and Fig. 5, for the custom-built rig and the TE, respectively.

One obvious observation is that 6-day-old fish F_2 and F_5 seem to be affected by repeated hits during the testing procedure, since the values computed for B_f and K_f exhibit abrupt changes from the 16th (custom-built rig), or the 11th (TE) test run onward. By the end of the 20th run, the fish muscular structure has seemingly been affected by repeated hitting, meaning that even if the fish is edible in aspects of retaining its sensory quality, its muscular internal structure has been compromised. The advantage of the currently proposed testing procedure is that the relevant values for B_f and K_f are indeed easy to be monitored throughout testing, making it possible to define the number of runs for which no

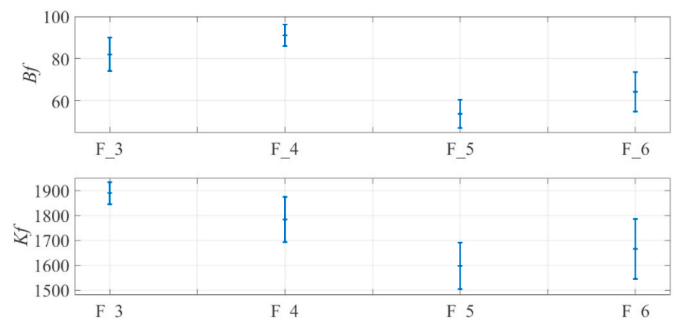


Fig. 7. Error-bars for B_f (top) and K_f (bottom) for F_3 - F_6 computed with data from test runs #1 - #10 in TE.

such damage to the fish has occurred. It is also reasonable that when a higher block release height (as in the TE case) is used, damage occurs earlier (at the 11th with TE instead of the 16th run with the custom-built rig). Abrupt changes in B_f and K_f values are easily noted when their mean and standard deviation are computed, as in Tables 2 and 3. The grey shaded cells in both tables indicate that standard deviation of B_f and K_f values is considerably lower when computed on data from up to the 15th (custom-built rig) or the 10th (TE) run.

Another remark is related to whether the differences in B_f and/or K_f values between fresh and 6-day-old fish are statistically significant. Fig. 6 presents the error-bars (mean \pm 2std) for B_f (top) and K_f (bottom) values computed on test data by the custom-built rig.

Whereas Fig. 7 shows similar information for B_f (top) and K_f (bottom) values computed on test data by the TE. The computed values for either B_f or K_f are not normally distributed. Hence, the error-bars showing two standard deviations do not correspond to 95% confidence level, but are purely indicative.

Nonetheless, it seems that 6-day-old fish exhibit significantly lower values for B_f than their fresh counterparts, since the relevant error-bars do not overlap in Fig. 6 (top) and Fig. 7 (top). On the other hand, it seems that 6-day-old fish exhibit values for K_f lower than those from fresh fish, even though this is more of a trend than a significant difference due to the overlapping in error-bars in Fig. 6 (bottom) and 7 (bottom). It is important that these results are similar to (and thus validate) those in the study (Dimogianopoulos & Grigorakis, 2017), which were established by using a different ramp-like testing protocol.

Finally, it is important to mention that the validation of rapid freshness evaluation methods usually requires correlation of results with those deriving from classic sensory, microbiological and biochemical freshness evaluation. Indeed, this analysis has been previously conducted with relevant results established in (Grigorakis & Dimogianopoulos, 2010; Dimogianopoulos & Grigorakis, 2011; 2014). Therein, a remarkably good correlation between our herein described methodology and the freshness stage of the fish as evaluated by sensory and chemical freshness has been demonstrated. Since this part of the work has already been done for the texture evaluation method in (Grigorakis & Dimogianopoulos, 2010; Dimogianopoulos & Grigorakis, 2011; 2014), the current study focused on the accomplishment of the testing protocol and algorithmic analysis of test data.

The herein-proposed fish texture evaluation method has shown successful description of the mechanical properties of the fish and their alterations. This can be effectively used for evaluating freshness in fish. The fact of recording early post-mortem changes in fish texture relating to onset and resolution of rigor mortis offers a significant advantage to our approach, over other rapid freshness evaluation methods that record changes, in conductivity or chemical status of the fish, since these become profound in later post-mortem times and relate to bacterial spoilage. Another advantage is that operation of the system is simple and can be applied in industrial environment. The limitation of the currently proposed method has mainly to do with the size/weight of the examined sample. The Texture Evaluation (TE) device developed to support our framework is such, in order to effectively operate with fish sizes between 300 g and 800 g-1 Kg, i.e. usual marketable sizes of common species of Mediterranean farmed fish (gilthead sea bream, sea bass). If evaluation of fish sizes other than those is required, perhaps the current system is inefficient in giving reliable measurements and respective modifications would be necessary to match different sizes.

4. Conclusion

The current work proposed an algorithm for operating within a nondestructive texture evaluation framework which may be

advantageously used in an industrial environment. The fish is part of a system which is dynamically loaded following a testing protocol designed to achieve favorable signal-to-noise values. At the same time, a new accurate closed-form analytical expression for the system response to the specific testing is comprehensively derived, and used along with experimental data, for computing specific mechanical properties of fish flesh, thus attributed to its freshness (viscoelasticity, springiness and so on). This only requires the use of conventional curve-fitting routines operating in the least-squares sense, found in most relevant software, such as MATLAB®. The algorithmic operational framework has been used for testing in a custom-built test rig and a prototype device, with results following remarkably similar trends, achieving clear distinction of differences in separate textural characteristics related to freshness, and consequently validating the proposed scheme.

CRedit authorship contribution statement

D. Dimogianopoulos: Fish testing, Formal analysis, Investigation, Writing - original draft, Funding acquisition. **K. Grigorakis:** Fish supply, testing, Data curation, writing, Funding acquisition.

Declaration of competing interest

The authors declare that there is no conflicts of interest.

Acknowledgements

This work was supported in part by FutureEUAqua project (Future growth in sustainable, resilient and climate friendly organic and conventional European aquaculture) funded by European Union's Horizon 2020 research and innovation program under grant agreement No 817737. The authors are particularly grateful to associates Mr. Emmanuel Tzevelekakis MSc who has been in charge for designing and building the Texture Evaluation device used for part of testing in this work and Dr. Panagiotis Christofilogiannis (AQUARK) for coordinating and providing the means for the Texture Evaluation device development.

References

- Cheng, J. H., Sun, D. W., Zeng, X. A., & Liu, D. (2015). Recent advances in methods and techniques for freshness quality determination and evaluation of fish and fish fillets: A review. *Critical Reviews in Food Science and Nutrition*, 55(7), 1012–1225. <https://doi.org/10.1080/10408398.2013.769934>
- Costa, C., D'Andrea, S., Russo, R., Antonucci, F., Pallottino, F., & Menesatti, P. (2011). Application of non-invasive techniques to differentiate sea bass (*Dicentrarchus labrax*, L. 1758) quality cultured under different conditions. *Aquaculture International*, 19, 765–778. <https://doi.org/10.1007/s10499-010-9393-9>
- Dimogianopoulos, D., & Grigorakis, K. (2011). A statistical model-based diagnostic scheme for cost-effective determination of freshness in fish industry. In *Proceedings of the 19th IEEE mediterranean conference on control & automation*. Institute of Electrical and Electronics Engineers. June 20-23, 2011, Corfu, Greece.
- Dimogianopoulos, D., & Grigorakis, K. (2014). Non-destructive textural assessment of fish freshness: A stochastic model-based approach robust to fish size variations. *Journal of Texture Studies*, 45(4), 274–287.
- Dimogianopoulos, D., & Grigorakis, K. (2017). Nondestructive semistatic testing methodology for assessing fish textural characteristics via closed-form mathematical expressions. *Journal of Food Quality*, 4852498. <https://doi.org/10.1155/2017/4852498>
- Dorf, R. C., & Bishop, R. H. (2010). *Modern control systems*. Upper Saddle River, New Jersey: Pearson Education Inc, ISBN 978-0136024583. Prentice Hall.
- European Food Safety Authority. (2009). Scientific opinion of the panel on animal health and welfare (Question N° EFSA-Q-2008-441): Species-specific welfare aspects of the main systems of stunning and killing of farmed seabass and seabream. *The EFSA Journal*, 10(10), 1–52. <https://efsa.onlinelibrary.wiley.com/doi/epdf/10.2903/j.efsa.2009.1010>.
- Freias, J., Vaz-Pires, P., & Câmara, J. S. (2020). From aquaculture production to consumption: Freshness, safety, traceability and authentication, the four pillars of quality. *Aquaculture*, 518, 734857.

- Grigorakis, K., & Dimogianopoulos, D. (2010). Cost-effective and non-destructive textural assessment of fish freshness via system identification principles. *Journal of Texture Studies*, 41(4), 492–510.
- Hassoun, A., & Karoui, R. (2017). Quality evaluation of fish and other seafood by traditional and nondestructive instrumental methods: Advantages and limitations. *Critical Reviews in Food Science and Nutrition*, 57, 1976–1998.
- Huss, H. H. (1988). *Fresh fish – quality and quality changes*, FAO fisheries series No. 29. Rome, Italy: FAO. 1988.
- Listrat, A., Lebet, B., Louveau, I., Astruc, T., Bonnet, M., Lefaucheur, L., ... Bugeon, J. (2016). How muscle structure and composition influence meat and flesh quality. *Science World Journal*, 3182746. <https://doi.org/10.1155/2016/3182746>, 2016.